



Title	The inhibitory effect of paclitaxel on (KV2.1) K <sup>+</sup> current in H9c2 cells
Author(s)	Kitamura, Naoko; Sakamoto, Kazuho; Ono, Tomoyuki; Kimura, Junko
Citation	Fukushima Journal of Medical Science. 61(1): 47-53
Issue Date	2015
URL	<a href="http://ir.fmu.ac.jp/dspace/handle/123456789/461">http://ir.fmu.ac.jp/dspace/handle/123456789/461</a>
Rights	© 2015 The Fukushima Society of Medical Science
DOI	10.5387/fms.2014-34
Text Version	publisher

[Original Article]

## THE INHIBITORY EFFECT OF PACLITAXEL ON (KV2.1) K<sup>+</sup> CURRENT IN H9c2 CELLS

NAOKO KITAMURA<sup>1</sup>, KAZUHO SAKAMOTO, TOMOYUKI ONO and JUNKO KIMURA

*Department of Pharmacology, Fukushima Medical University, School of Medicine, Fukushima, Japan*

(Received December 17, 2014, accepted March 17, 2015)

**Abstract** : Using the whole-cell voltage clamp technique, we investigated the effect of paclitaxel, an anticancer agent which promotes microtubule formation, on K<sup>+</sup> current in H9c2 cells originated from rat embryonic cardiac myocytes. Paclitaxel inhibited Kv2.1 voltage-dependent K<sup>+</sup> current (IKur) with ultra-rapidly activating and slowly inactivating kinetics in a concentration-dependent manner. The inhibitory effect of paclitaxel on IKur was time-dependent and more marked at 200 ms after the onset than at the beginning of the depolarizing pulse. The IC<sub>50</sub> value of paclitaxel was 1.1 μM at 200 ms. The time-dependent inhibition suggests that paclitaxel might be an open channel blocker of Kv2.1. This inhibition of Kv2.1 may be involved in the adverse effects of paclitaxel on cardiac and neuronal cells.

**Key words** : paclitaxel, Kv2.1, K<sup>+</sup> current, H9c2 cells, whole-cell clamp

### INTRODUCTION

Paclitaxel (Fig. 1) is an alkaloid ester derived from Pacific yew (*Taxus brevifolia*)<sup>1</sup> and is used for chemotherapy of various cancers including ovarian, gastric, and lung cancers (for review see<sup>2</sup>). Moreover, paclitaxel binds to microtubules with a high affinity to enhance tubulin polymerization<sup>3,4</sup>, thus preventing microtubule depolymerization and consequently inhibits cancer cell division<sup>5,6</sup>. It has been shown in HeLa cells that paclitaxel blocks the G2/M phase cell cycle<sup>7,8</sup>.

On the other hand, paclitaxel has serious adverse reactions including hypersensitivity, neutropenia, peripheral neuropathy, and cardiac conduction disorder<sup>2</sup>. Peripheral neuropathy and cardiac conduction disorder are two especially serious adverse effects of paclitaxel, which reduce the quality of life and the activity of daily life of patients and make chemotherapy difficult to continue. In neuroblastoma SH-SY5Y cells, an inositol-3-phosphate-mediated reduction in Ca<sup>2+</sup> signaling was suggested to be involved in paclitaxel-induced peripheral neuropathy<sup>9</sup>. In rat cardiac ventricular cells, taxol was

found to reduce the amplitude of contraction and the Ca<sup>2+</sup> transient without a significant change in the L-type Ca<sup>2+</sup> channel<sup>10,11</sup>. However, the detailed mechanism of the adverse effects of paclitaxel is unknown.

In order to clarify this mechanism, we examined the effects of paclitaxel on the K<sup>+</sup> current in H9c2 cells. H9c2 cells are derived from embryonic rat heart tissue and often used as a model of cardiac myocytes<sup>12</sup>. Also, H9c2 cells have IKur, an ultra-rapidly activating and slowly inactivating voltage-gated delayed rectifier K<sup>+</sup> current, which is attributed to the Kv2.1 gene<sup>13-16</sup>. This current is sensitive to various drugs, including thiopental<sup>15</sup> and isoliquiritigenin<sup>17</sup>, a component of licorice.

Kv2.1 is ubiquitously expressed in the rat brain and peripheral neurons<sup>18</sup> as well as in heart, and its protein expression is known to occur in human atria<sup>19</sup>. We therefore tested the effect of paclitaxel on IKur in H9c2 cells. In this report, we demonstrate that an acute administration of paclitaxel inhibits IKur in H9c2 cells in a unique, time-dependent manner.

Corresponding author : Junko Kimura E-mail : jkimura@fmu.ac.jp

<https://www.jstage.jst.go.jp/browse/fms> <http://www.fmu.ac.jp/home/lib/F-igaku/>

<sup>1</sup>Present address : Naoko Kitamura, Department of Pharmaceutical Science, Tohoku University Hospital, Sendai, 980-8574, Japan

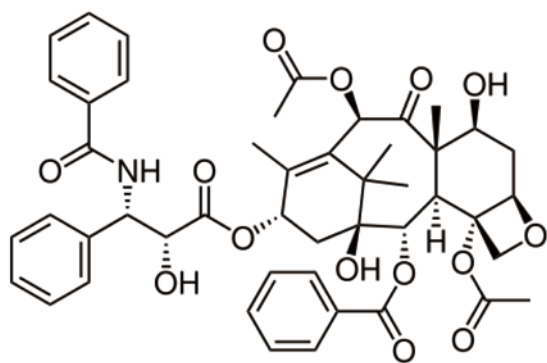


Fig. 1. Chemical structure of paclitaxel.

## MATERIALS AND METHODS

### Cell culture

H9c2 cells (purchased from Dainippon Sumitomo Seiyaku, Osaka) were maintained in Dulbecco's modified Eagle's medium (Sigma, St. Louis, MO, U.S.A.) supplemented with 5% fetal bovine serum in a humidified atmosphere of 10% CO<sub>2</sub> and 90% air at 37°C. For electrophysiological recordings, cells were displaced from the culture dish by using Ca<sup>2+</sup> free EDTA-containing Ringer solution. The cells were used after 3–5 days of culture.

### Patch-clamp recording

Membrane currents were recorded by the whole-cell patch clamp method<sup>20</sup>. H9c2 cells were placed in a recording chamber attached to the stage of an inverted microscope (Model 80121, Nikon, Tokyo). The cells were superfused with Tyrode's solution at a rate of 1 mL/min. The temperature of the bath solution was maintained at 35 ± 0.5°C with a water jacket. Patch pipettes were forged from 1.5 mm diameter glass capillaries (Nihon Rikagaku Kikai, Tokyo) with a microelectrode puller (pp-83, Narishige, Tokyo). The pipette resistance was 3–6 MΩ when filled with the pipette solution. The solution contained (in mM): 120 KOH, 20 KCl, 3 MgCl<sub>2</sub>, 5 MgATP, 20 HEPES (4-(2-hydroxyethyl)-1-piperazine-ethanesulfonic acid), 10 EGTA (ethylene glycol bis(2-aminoethylether)tetraacetic acid), and 50 aspartic acid (pH 7.2 with aspartic acid). Tyrode's solution contained (in mM): 140 NaCl, 5.4 KCl, 1.8 CaCl<sub>2</sub>, 1 MgCl<sub>2</sub>, 0.33 NaH<sub>2</sub>PO<sub>4</sub>, 5.5 glucose, and 5 HEPES (pH 7.4 with NaOH). The electrode was connected to a patch-clamp amplifier (CEZ-2400, Nihon Kohden, Tokyo). Recording signals were filtered at a 2.5-kHz bandwidth, and the series resistance was compensated. Membrane currents were recorded using pCLAMP8 software (Axon In-

struments, Foster City, CA, U.S.A.). Depolarizing voltage pulses of 200-ms or 3-s duration were given with 10-mV steps every 10 s from the holding potential (HP) of -60 mV. Current signals were stored online and analyzed by a computer (GX150, OPTIPLEX, Dell, TX, U.S.A.).

### Drugs

Paclitaxel purchased from Sigma was made up as a 100-mM stock solution in dimethyl sulfoxide (DMSO), which was diluted in Tyrode's solution immediately prior to use. The final concentration of DMSO was <0.1%, which did not affect the K<sup>+</sup> current. All the chemicals were of the highest grade available.

### Data analysis

All the values were presented as means ± SE of the mean (number of experiments). The percentage inhibition of K<sup>+</sup> current was measured at 60 mV at various concentrations of paclitaxel. The IC<sub>50</sub> (concentration for 50% inhibition) and the Hill coefficient values were obtained using Origin ver. 6J (Microcal Software, Inc., U.S.A.). Statistical significance was evaluated using one-way ANOVA and then Dunnett T3 test as a post ad hoc test for comparison between the currents before and after paclitaxel application (Fig. 4, control vs paclitaxel). Student's paired T test was used between the peak current and the current at 200 ms (see Fig. 4, Peak vs 200 ms), and for comparison between the half time of the current before and after paclitaxel application (Fig. 6).

## RESULTS

### Inhibitory effect of paclitaxel on K<sup>+</sup> current

In the H9c2 cells, an outward K<sup>+</sup> current was elicited by a series of depolarizing square voltage pulses with a 200 ms duration from -60 mV HP to a voltage range between -50 mV to 60 mV (Fig. 2A). Perfusing 100 μM paclitaxel for 5 min suppressed this K<sup>+</sup> outward current dramatically (Fig. 2B). The inhibitory effect of paclitaxel was irreversible at least during 10 min of washing off the drug. Fig. 3 illustrates the current-voltage relationships measured at the peak (A) and at the end of 200-ms (B) voltage pulses of control (open symbols) and in the presence of paclitaxel (filled symbols). The data from 5 cells were averaged and normalized in order to compare the effect of paclitaxel between the peak and at 200 ms of IKur

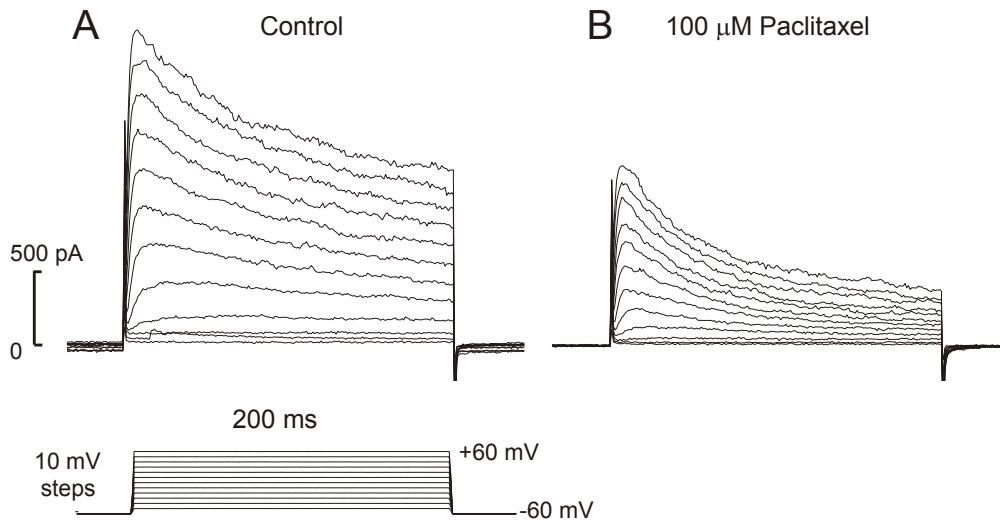


Fig. 2. Inhibitory effect of paclitaxel on  $I_{Kur}$  of an H9c2 cell. A. Control currents in response to depolarizing pulses of 200-ms durations. The superimposed voltage pulses are illustrated below the currents. B. Currents recorded in the presence of 100  $\mu$ M paclitaxel.

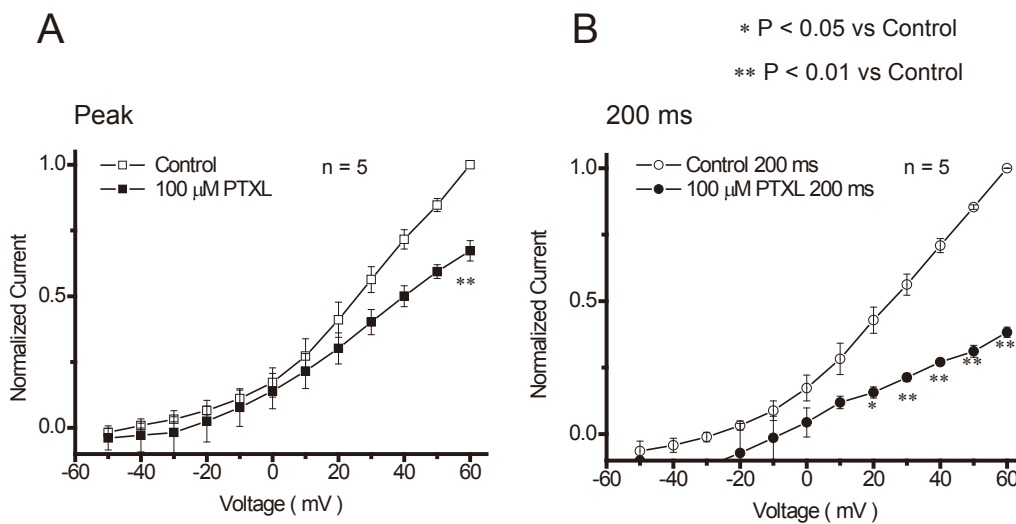


Fig. 3. I-V curves of peak (A) and at the end of 200 ms (B) in the absence (open symbols) and presence (filled symbols) of 100  $\mu$ M paclitaxel (PTXL). The currents were averaged and normalized in 5 cells.

(Fig. 3). Paclitaxel at 100  $\mu$ M inhibited the peak current by  $38.3 \pm 1.9\%$  ( $n = 5$ ), whereas the current at 200 ms by  $67.2 \pm 3.9\%$  ( $n = 5$ ) at 60 mV. Thus, the current at 200 ms was inhibited more extensively than that at the peak. These results suggest that the suppression of  $I_{Kur}$  by paclitaxel was time dependent.

*Concentration-dependent effect of paclitaxel on  $I_{Kur}$*

To obtain a concentration-inhibition curve of paclitaxel, various concentrations of paclitaxel were applied, and the current magnitude was measured at 60 mV at the peak and at the end of the 200-ms pulses (Fig. 4). The percentage inhibition of the

K<sup>+</sup> current was calculated with respect to each control value. We employed paclitaxel concentrations from 0.01  $\mu$ M, which is within the therapeutic range, to a high concentration of 100  $\mu$ M. Paclitaxel inhibition was concentration dependent and significant inhibition was detected at 1  $\mu$ M and 100  $\mu$ M paclitaxel compared to the control current before application of paclitaxel. The inhibition of the current at the peak almost reached the maximum effect of 10–30% of the control in the concentration range up to 100  $\mu$ M paclitaxel. However, the current at 200 ms was reduced to about 60% by 100  $\mu$ M paclitaxel, and the effect did not appear to have reached the maximum. Therefore, paclitaxel suppressed  $I_{Kur}$  at 200

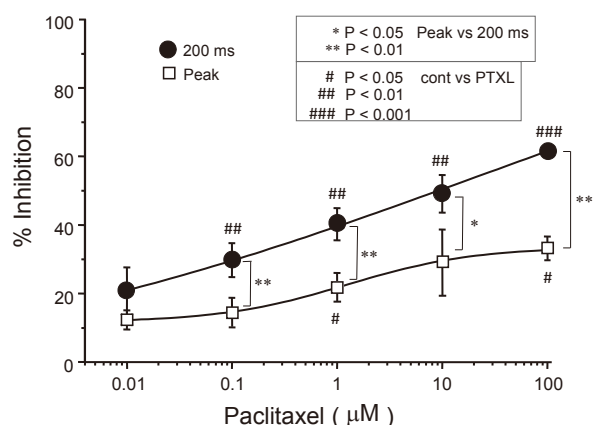


Fig. 4. Concentration-inhibition curves of 100  $\mu\text{M}$  paclitaxel. The peak currents (open squares) of  $I_{\text{Kur}}$  and the currents at the end of 200-ms pulses (filled circles) were measured, and the difference were divided by the control to obtain the % inhibition by paclitaxel. The values were averaged from 4 or 5 cells. Statistical significance was compared between % inhibitions by paclitaxel at the peak and at 200 ms (\* $P < 0.05$ , \*\* $P < 0.01$ ), and % inhibitions before (0 %) and after paclitaxel application (# $P < 0.05$ , ## $P < 0.01$ , ### $P < 0.001$ ).

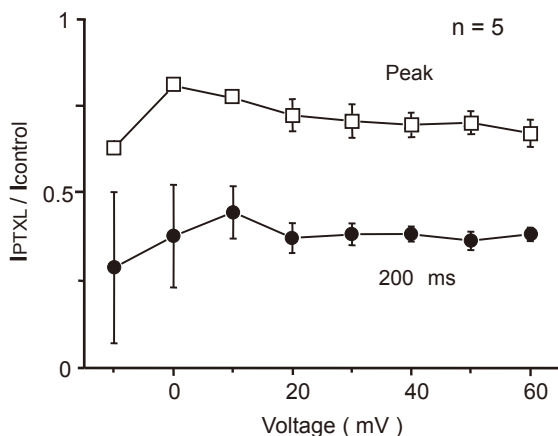


Fig. 5. Voltage dependency is not apparent in the inhibitory effect of 100  $\mu\text{M}$  paclitaxel on  $I_{\text{Kur}}$ . The ratios between the currents in the presence ( $I_{\text{PTXL}}$ ) and absence ( $I_{\text{control}}$ ) of paclitaxel at each voltage are plotted for the peak (open squares) and at the end of 200-ms pulses (filled circles).

ms significantly stronger than that at the peak at four out of five concentrations we tested. The  $\text{IC}_{50}$  value of paclitaxel at 200 ms was approximately 1.1  $\mu\text{M}$ .

#### Voltage dependency of the inhibitory effect of paclitaxel

We examined whether the inhibitory effect of paclitaxel on  $I_{\text{Kur}}$  was voltage dependent. Using the data in Fig. 3, the ratio of the current between in the presence ( $I_{\text{PTXL}}$ ) and in the absence ( $I_{\text{cont}}$ ) of 100

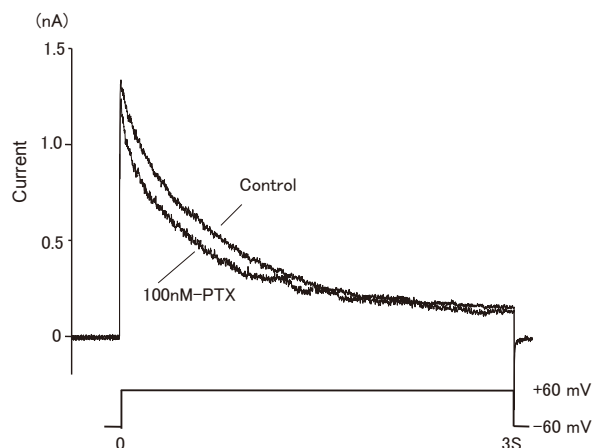


Fig. 6. Representative data of superimposed currents in response to 3-s depolarizing pulses in the absence and presence of 0.1  $\mu\text{M}$  paclitaxel. The half-time of inactivation of the current is 378 ms in the absence of paclitaxel in contrast to 266 ms in the presence of paclitaxel.

$\mu\text{M}$  paclitaxel was calculated both at the peak and at 200 ms. The average values of the ratio were plotted in the current ratio voltage curves in Fig. 5, which indicated that the inhibitory effect of paclitaxel was greater at 200 ms than that at the peak of  $I_{\text{Kur}}$  at all the potentials examined. However, the inhibitory effect of paclitaxel was not voltage dependent.

#### Time-dependent effect of paclitaxel on $I_{\text{Kur}}$

The time-dependent inhibitory effect of paclitaxel was evaluated with a longer depolarization pulse of a 3-s duration because the inactivation of  $I_{\text{Kur}}$  was so slow that it had not yet reached a steady state at 200 ms<sup>15</sup>. In this series of experiment, a low concentration of 0.1  $\mu\text{M}$  paclitaxel was employed because it did not dramatically change the peak  $I_{\text{Kur}}$ , although it should have disclosed the time-dependent change clearly during the inactivation. To demonstrate the effect of 0.1  $\mu\text{M}$  paclitaxel, we superimposed  $I_{\text{Kur}}$  in response to a depolarizing pulse of 3-s duration in the absence and presence of paclitaxel in a H9c2 cell. The pulse was depolarised from  $-60$  mV HP to  $60$  mV. In the representative data in Fig. 6, the half-time of  $I_{\text{Kur}}$  inactivation ( $T_{1/2}$ ) was 378 ms in control, whereas it was 266 ms in the presence of paclitaxel. The average  $T_{1/2}$  value obtained from 6 different cells was  $447 \pm 27$  ms in the control and  $321 \pm 40$  ms ( $n = 6$ ,  $p < 0.05$ ) in the presence of 0.1  $\mu\text{M}$  paclitaxel. We concluded that paclitaxel inhibited  $I_{\text{Kur}}$  by accelerating  $I_{\text{Kur}}$  inactivation.

DISCUSSION

In the present study, we found that paclitaxel inhibited I<sub>Kur</sub> in H9c2 cells irreversibly and in a concentration-dependent manner. The highest concentration of paclitaxel we used was 100 μM, which inhibited the peak I<sub>Kur</sub> at 60 mV to 67.3 ± 3.9% (*n* = 5) of the control, whereas it inhibited I<sub>Kur</sub> at 200-ms quasi-steady state to 38.3 ± 1.9% (*n* = 5) of the control. Therefore, paclitaxel inhibited I<sub>Kur</sub> in a time-dependent manner, and the inhibition was stronger at 200 ms than that at the peak. The IC<sub>50</sub> value of paclitaxel at 200 ms was 1.1 μM. We could not detect the IC<sub>50</sub> value at the peak I<sub>Kur</sub> because the inhibition of paclitaxel did not reach the maximum at 100 μM. The minimum concentration of paclitaxel that started to inhibit I<sub>Kur</sub> at 200 ms was 0.1 μM (*p* < 0.05, see Fig. 4). This concentration was within the therapeutic range of paclitaxel, 0.01 to 0.1 μM. Therefore, there is a possibility that paclitaxel inhibits I<sub>Kur</sub> at clinical concentrations.

Paclitaxel at 0.1 μM did not significantly reduce I<sub>Kur</sub> peak but shortened the inactivation process of I<sub>Kur</sub> from control T<sub>1/2</sub> 447 ± 27 ms to 321 ± 40 ms (*n* = 6, *p* < 0.05). The most common effect of paclitaxel is a transient asymptomatic bradycardia, which was noted in 29% of the patients participating in one trial<sup>2)</sup>. More serious bradyarrhythmias, including Mobitz type I (Wenckebach's syndrome), Mobitz type II, and third-degree heart block, have been noted in 0.1% of patients enrolled in trials that required continuous cardiac monitoring<sup>2)</sup>. In the human heart, Kv2.1 and Kv1.5 are expressed as I<sub>Kur</sub> genes in atria<sup>21,22)</sup>. In H9c2 cells, the expression of Kv2.1 mRNA was detected but not that of Kv1.5<sup>16)</sup>. I<sub>Kur</sub> is activated during the plateau phase of the action potential and contributes to repolarization. If the I<sub>Kur</sub> peak current is inhibited and the decay time is shortened, the duration of the action potential is prolonged, so that the absolute refractory phase of the action potential may be extended. This may cause the delay of conduction in the atrium and Purkinje fibers. In addition, triggered activity such as early afterdepolarization may occur during the prolonged repolarization phase. These may induce cardiac arrhythmia and conduction disorder as a result of an effect of paclitaxel.

In human, Kv2.1 was found not only in the heart but also in the pulmonary artery<sup>23)</sup>. Inhibition of Kv2.1 in rat pulmonary artery led to depolarization of vascular smooth muscle<sup>24)</sup>. Depolarization of the pulmonary blood vessel at the atrial boundary

region might also trigger arrhythmia. A significant focal stenosis was reported in the coronary artery treated with a paclitaxel-eluting stent<sup>25)</sup>. There may be a relation between the depolarization of arterial smooth muscle by paclitaxel and facilitating arterial stenosis.

Antiarrhythmic drugs, such as quinidine and disopyramide, also suppress I<sub>Kur</sub><sup>26,27)</sup>. Suzuki *et al.*<sup>15)</sup> found that thiopental suppressed I<sub>Kur</sub> in H9c2 cells. However, these I<sub>Kur</sub> inhibitors differ from paclitaxel because their inhibitory action was not time dependent. Therefore, the site of action must be different between paclitaxel and the other inhibitors including thiopental. Kv2.1 is a voltage-gated potassium (Kv) channel α subunit expressed in mammalian heart, brain, and peripheral nervous system. Multiple modulatory protein molecules of Kv2.1 are known, including MinK (or KCNE1), MinK-related peptides (MiRPs or KCNE2). Modulatory subunits for Kv2.1 also include electrically silent Kv α subunits such as Kv5.1, Kv6.1, Kv8.1, Kv9.1-9.3, and KChAP ancillary subunit<sup>28)</sup>. Therefore, there is a possibility that paclitaxel binds not with the Kv2.1 α subunit but with those modifying molecules, and changes the kinetics of I<sub>Kur</sub> in H9c2 cells. There is also a possibility that paclitaxel is an open channel blocker of Kv2.1.

Recently, T-type Ca<sup>2+</sup> channel inhibitors were found to inhibit paclitaxel-evoked neuropathy<sup>29)</sup>. T-type Ca<sup>2+</sup> channels are involved in the action potential of the sinoatrial pacemaker cells in the heart<sup>30)</sup>. If T-type Ca<sup>2+</sup> channels are accelerated by paclitaxel, the sinus rhythm may become tachycardia rather than bradycardia. The most common cardiac effect of paclitaxel is bradyarrhythmia; therefore, T-type Ca<sup>2+</sup> channels may not be a major target of paclitaxel. However, various other disturbances related with paclitaxel were described including myocardial infarction, cardiac ischemia, atrial arrhythmia, and ventricular tachycardia<sup>2)</sup>. The most serious toxicity may be an increased frequency of cardiac toxicity of anthracyclines including doxorubicin in patients treated with paclitaxel<sup>2)</sup>. Decrease in Ca<sup>2+</sup> release from the sarcoplasmic reticulum by paclitaxel may be related to the increment of anthracycline toxicity during the combination chemotherapy<sup>11)</sup>.

Kv2.1 is expressed not only in the heart but also in the central and peripheral nervous system, blood vessels, and pancreatic beta cells<sup>31-33)</sup>. Paclitaxel may also show an inhibitory effect on Kv2.1 in those tissues. Kv2.1 suppression increases firing frequency in neurons and in pancreatic beta cells<sup>34-36)</sup>. However, it is unknown what functional change may

occur in those tissues as a result.

We conclude that paclitaxel acutely suppresses Kv2.1 at a concentration higher than 0.1  $\mu\text{M}$ , which might induce cardiac conduction and peripheral nerve disorders. Further examination is necessary to clarify the effect and its mechanism.

#### ACKNOWLEDGEMENT

This work was supported by grants-in-aid No. 21590288 and 024590325 for JK and 25460338 for KS from Japan Society for Promotion of Science. We thank Ms. Sanae Sato for her technical assistance.

#### CONFLICT OF INTEREST

We have no conflict of interest to disclose.

#### REFERENCES

1. Wani MC, Taylor HL, Wall ME, Coggon P, MacPhail AT. Plant antitumor agents. VI. The isolation and structure of taxol, a novel antileukemic and antitumor agent from *Taxus brevifolia*. *J Am Chem Soc*, **93** : 2325-2327, 1971.
2. Rowinsky EK, Donehower RC, Paclitaxel (taxol). *N Engl J Med*, **332** : 1004-1014, 1995.
3. Schiff PB, Fant J, Horwitz SB. Promotion of microtubule assembly in vitro by taxol. *Nature*, **277** : 665-667, 1979.
4. Kumar N. Taxol-induced polymerization of purified tubulin. Mechanism of action. *J Biol Chem*, **256** : 10435-10441, 1981.
5. Schiff PB, Horwitz SB. Taxol stabilizes microtubules in mouse fibroblast cells. *Proc Natl Acad Sci USA*, **77** : 1561-1565, 1980.
6. Wilson L, Miller HP, Farrell KW, Snyder KB, Thompson WC, Purich DL. Taxol stabilization of microtubules in vitro : dynamics of tubulin addition and loss at opposite microtubule ends. *Biochemistry*, **24** : 5254-5262, 1985.
7. Hornback NB, Shen RN, Sutton GP, Shidnia H, Kaiser HE. Synergistic cytotoxic and antitumor effects of irradiation and taxol on human HeLa cervix carcinoma and mouse B16 melanoma cells. *In Vivo*, **8** : 819-823, 1994.
8. Jordan MA, Wendell K, Gardiner S, Derry WB, Copp H, Wilson L. Mitotic block induced in HeLa cells by low concentrations of paclitaxel (Taxol) results in abnormal mitotic exit and apoptotic cell death. *Cancer Res*, **56** : 816-825, 1996.
9. Boehmerle W, Zhang K, Sivula M, Heidrich FM, Lee Y, Jordt SE, Ehrlich BE. Chronic exposure to paclitaxel diminishes phosphoinositide signaling by calpain-mediated neuronal calcium sensor-1 degradation. *Proc Natl Acad Sci U S A*, **104** : 11103-11108, 2007.
10. Galli A, DeFelice LJ. Inactivation of L-type Ca channels in embryonic chick ventricle cells : dependence on the cytoskeletal agents colchicine and taxol. *Biophys J*, **67** : 2296-2304, 1994.
11. Howarth FC, Calaghan SC, Boyett MR, White E. Effect of microtubule polymerizing agent taxol on contraction,  $\text{Ca}^{2+}$  transient and L-type  $\text{Ca}^{2+}$  current in rat ventricular myocytes. *J Physiol*, **516** : 409-419, 1999.
12. Kimes BW, Brandt BL. Properties of a clonal muscle cell line from rat heart. *Experimental Cell Research*, **98** : 367-381, 1976.
13. Shi H, Wang H, Han H, Xu D, Yang B, Nattel S, Wang Z. Ultrarapid delayed rectifier  $\text{K}^+$  current in H9c2 rat ventricular cell line : biophysical property and molecular identity. *Cell Physiol Biochem*, **12** : 215-226, 2002.
14. Wang W, Hino N, Yamasaki H, Aoki T, Ochi R.  $\text{K}_v2.1$   $\text{K}^+$  channels underlie major voltage-gated  $\text{K}^+$  outward current in H9c2 myoblasts. *Jpn J Physiol*, **52** : 507-514, 2002.
15. Suzuki H, Momoi N, Ono T, Maeda S, Shikama Y, Matsuoka I, Suzuki H, Kimura J. Inhibitory effect of thiopental on ultra-rapid delayed rectifier  $\text{K}^+$  current in H9c2 cells. *J Pharmacol Sci*, **99** : 177-184, 2005.
16. Suganami A, Sakamoto K, Ono T, Watanabe H, Hijioka N, Murakawa M, Kimura J. The inhibitory effect of Shakyakukanzoto on  $\text{K}^+$  current in H9c2 cells. *Fukushima J Med Sci*, **60** : 1-9, 2013.
17. Noguchi C, Yang J, Sakamoto K, Maeda R, Takahashi K, Ono T, Murakawa M, Kimura J. Inhibitory effects of isoliquiritigenin and licorice extract on voltage-dependent  $\text{K}^+$  currents in H9c2 cells. *J Pharmacol Sci*, **108** : 439-445, 2008.
18. Malin SA, Nerbonne JM. Delayed rectifier  $\text{K}^+$  currents, IK, are encoded by  $\text{Kv}2$   $\alpha$ -subunits and regulate tonic firing in mammalian sympathetic neurons. *J Neurosci*, **22** : 10094-10105, 2002.
19. Van Wagoner DR, Pond AL, McCarthy PM, Trimmer JS, Nerbonne JM. Outward  $\text{K}^+$  current densities and  $\text{Kv}1.5$  expression are reduced in chronic human atrial fibrillation. *Circ Res*, **80** : 772-781, 1997.
20. Hamill OP, Marty A, Neher E, Sakmann B, Sigworth FJ. Improved patch-clamp techniques for high-resolution current recording from cells and cell-free membrane patches. *Pflugers Arch*, **391** : 85-100, 1981.
21. Tamkun MM, Knoth KM, Walbridge JA, Kroemer H, Roden DM, Glover DM. Molecular cloning and characterization of two voltage-gated  $\text{K}^+$  chan-

- nel cDNAs from human ventricle. *FASEB J*, **5** : 331-337, 1991.
22. Antzelevitch C, Dumaine R. Electrical heterogeneity in the heart : physiological, pharmacological, and clinical implications. In : *Handbook of Physiology. The Heart*. Bethesda, Am Physiol Soc, 654-692, 2001.
  23. Yuan XJ, Wang J, Juhaszova M, Golovina VA, Rubin LJ. Molecular basis and function of voltage-gated K<sup>+</sup> channels in pulmonary arterial smooth muscle cells. *Am J Physiol*, **274** : L621-635, 1998.
  24. Archer SL, Souil E, Dinh-Xuan AT, Schremmer B, Mercier JC, El Yaagoubi A, Nguyen-Huu L, Reeve HL, Hampl V. Molecular identification of the role of voltage-gated K<sup>+</sup> channels, Kv1.5 and Kv2.1, in hypoxic pulmonary vasoconstriction and control of resting membrane potential in rat pulmonary artery myocytes. *J Clin Invest*, **101** : 2319-2330, 1998.
  25. Kim JW, Park CG, Seo HS, Oh DJ. Delayed severe multivessel spasm and aborted sudden death after Taxus stent implantation. *Heart*, **91** : e15, 2005.
  26. Feng J, Wang Z, Li GR, Nattel S. Effects of class III antiarrhythmic drugs on transient outward and ultra-rapid delayed rectifier currents in human atrial myocytes. *J Pharmacol Exp Ther*, **281** : 384-392, 1997.
  27. Sanchez - Chapula JA, Mechanism of transient outward K<sup>+</sup> channel block by disopyramide. *J Pharmacol Exp Ther*, **290** : 515-523, 1999.
  28. McCrossan ZA, Roepke TK, Lewis A, Panaghie G, Abbott GW. Regulation of the Kv2.1 potassium channel by MinK and MiRP1. *J Membr Biol*, **228** : 1-14, 2009.
  29. Okubo K, Takahashi T, Sekiguchi F, Kanaoka D, Matsunami M, Ohkubo T, Yamazaki J, Yamazaki J, Fukushima N, Yoshida S, Kawabata A. Inhibition of t-type calcium channels and hydrogen sulfide-forming enzyme reverses paclitaxel-evoked neuropathic hyperalgesia in rats. *Neuroscience* **188** : 148-156, 2011.
  30. Hagiwara N, Irisawa H, Kameyama M. Contribution of two types of calcium currents to the pacemaker potentials of rabbit sino-atrial node cells. *Journal of Physiology*, **395** : 233-253, 1988.
  31. Xu C, Lu Y, Tang G, Wang R. Expression of voltage-dependent K<sup>+</sup> channel genes in mesenteric artery smooth muscle cells. *Am J Physiol*, **277** : G1055-1063, 1999.
  32. MacDonald PE, Ha XF, Wang J, Smukler SR, Sun AM, Gaisano HY, Salapatek AM, Backx PH, Wheeler MB. Members of the Kv1 and Kv2 voltage-dependent K<sup>+</sup> channel families regulate insulin secretion. *Mol Endocrinol*, **15** : 1423-1435, 2001.
  33. Jacobson DA, Kuznetsov A, Lopez JP, Kash S, Ammälä CE, Philipson LH. Kv2.1 ablation alters glucose-induced islet electrical activity, enhancing insulin secretion. *Cell Metab*, **6** : 229-235, 2007.
  34. Murakoshi H, Trimmer JS. Identification of the Kv2.1 K<sup>+</sup> channel as a major component of the delayed rectifier K<sup>+</sup> current in rat hippocampal neurons. *J Neurosci*, **19** : 1728-1735, 1999.
  35. Tsantoulas C, Zhu L, Yip P, Grist J, Michael GJ, McMahon SB. Kv2 dysfunction after peripheral axotomy enhances sensory neuron responsiveness to sustained input. *Exp Neurol*, **251** : 115-126, 2014.
  36. Tamarina NA, Kuznetsov A, Fridlyand LE, Philipson LH. Delayed-rectifier (KV2.1) regulation of pancreatic beta-cell calcium responses to glucose : inhibitor specificity and modeling. *Am J Physiol Endocrinol Metab*, **289** : E578-585, 2005.